

# Frequency Domain Analysis for An Adaptive Windowing Parabolic Sliding Mode Filter

Shanghai Jin<sup>1</sup>, Xiaodan Wang<sup>1</sup>, Yonggao Jin<sup>1</sup> and Xiaogang Xiong<sup>2</sup>

<sup>1</sup>School of Engineering, Yanbian University, Yanji 133002, China

<sup>2</sup>Singapore Institute Of Manufacturing Technology, 71 Nanyang Dr, Singapore 638075, Singapore

**Abstract.** This paper analyses a frequency domain performance of an adaptive windowing parabolic sliding mode filter (AW-PSMF) by using Describing Function method. The analysis results show that AW-PSMF has similar gain characteristics to that of the second-order Butterworth low-pass filter (2-LPF), but AW-PSMF produces flatter gain behaviour than 2-LPF does at cutoff frequency. In addition, AW-PSMF produces smaller phase lag than 2-LPF does.

## 1 Introduction

In feedback control of mechatronic systems, feedback signals are usually corrupted by noise. Thus, a filter is required for removing noise from feedback signals. Linear filters are commonly applied for reducing noise because of their simplicity. However, in a linear filter, any noise component is proportionally transferred into the output. In addition, a large phase lag, which may result in the instability of feedback systems, is caused by strong noise attenuation.

Nonlinear filters have been applied for avoiding drawbacks of linear filters. For example, median filters [1] are used for removing high-frequency noise, but they are computationally expensive [2]. As another example, stochastic filters, e.g., Kalman filter [3], [4], are also applied in some applications. However, a dynamics model of the source of the signal, which is usually not available, is required. In addition, their performance depends on the model accuracy.

In the last decade, sliding mode observers based on the super-twisting algorithm [5], [6] has been attracted much attention. One advantage of these observers is that they theoretically realize finite time convergence in continuous-time analysis. However, typically with finite difference, the convergence accuracy in discrete-time implementation depends on the sampling period, as reported in [5]. Moreover, they are prone to overshoot during the convergence. Furthermore, they also require a system dynamics model.

The sliding mode filter that employs a parabolic sliding surface has been studied [7], [8]. One of major advantages of this filter is that, in the case of a constant input is provided, the output converges to the input in finite time. However, the filter is prone to overshoot. In addition, the discrete-time implementation of the filter

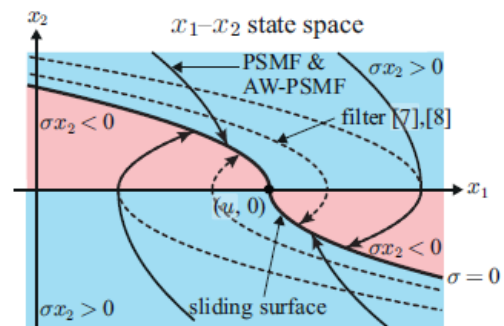


**Figure 1.** The parabolic-shaped sliding surface (thick solid curve) and trajectories of the state of PSMF and AW-PSMF (thin solid curve) and the filter [7], [8] (thin dotted curve).

produces high-frequency chattering due to inappropriate discretization.

Toward to the drawbacks of the parabolic sliding mode filter [7], [8], Jin *et al.* [9] presented a new parabolic sliding mode filter, which is referred to PSMF, for effectively removing noise in feedback control systems. It is reported in [9] that PSMF produces smaller phase lag than linear filters, and it is less prone to overshoot than the sliding mode filter [7], [8]. In addition, the algorithm of PSMF, which is derived by using the backward Euler differentiation, does not produce chattering. After that, Jin *et al.* [10] presented an adaptive windowing parabolic sliding mode filter, which is named as AW-PSMF, by extending PSMF. It is stated in [10] that AW-PSMF adaptively adjusts its window size for obtaining the largest window size that optimizes the trade-off between the filtering smoothness and the delay suppression. The effectiveness of AW-PSMF has been experimentally validated in feedback control of a mechatronic system. In [10], however, the frequency domain performance of AW-PSMF is not evaluated.

This paper presents a frequency domain performance of AW-PSMF. It is shown that AW-PSMF has similar gain characteristics to that of the second-order Butterworth low-pass filter (2-LPF), but AW-PSMF produces smaller phase lag (maximum 140 degree) than 2-LPF (maximum 180 degree) does.

The rest of this paper is organized as follows. Section 2 provides a brief overview of parabolic sliding mode filters. Section 3 analysis the performance of AW-PSMF in frequency domain. Section 4 gives concluding remarks.

## 2 Parabolic sliding mode filters

In [9], Jin *et al.* presented a parabolic sliding mode filter (PSMF), of which continuous-time expression is given as follows:

$$\dot{x}_1 = x_2 \quad (1a)$$

$$\dot{x}_2 \in -\frac{F(H+1)}{2} \text{sgn}(\sigma(F, u, x_1, x_2)) - \frac{F(H-1)}{2} \text{sgn}(x_2), \quad (1b)$$

where

$$\sigma(F, u, x_1, x_2) \triangleq 2F(x_1 - u) + |x_2| x_2. \quad (2)$$

Here,  $u$  is the input,  $x_1$  and  $x_2$  are the outputs, and  $F > 0$  and  $H > 1$  are constants. In addition,  $\text{sgn}()$  is the set-valued signum function defined as follows:

$$\text{sgn}(z) \triangleq \begin{cases} 1 & \text{if } z > 0 \\ [-1, 1] & \text{if } z = 0 \\ -1 & \text{if } z < 0 \end{cases} \quad (3)$$

It should be noted that  $\text{sgn}(z)$  returns a set instead of a single value when  $z = 0$ .

Figure 1. illustrates the sliding surface and state trajectories of PSMF in  $x_1$ - $x_2$  space. It is shown that PSMF employs a parabolic-shaped sliding surface, and the state is attracted to the sliding surface from both sides, whereas as the state of the filter [7][8] moves in parallel to the sliding surface in the regions of  $\sigma x_2 > 0$ . Such an advantage of PSMF can be attributed to the use of  $H > 1$ .

In [9], Jin *et al.* also provided the following PSMF's discrete-time algorithm, which is derived by using the backward Euler discretization:

### Algorithm PSMF

$$x_2^*(k) := FT\Phi\left(\frac{u(k) - x_1(k-1)}{FT^2}\right) \quad (4a)$$

$$x_2(k) := \text{clip}(\text{clip}(x_2(k-1) - HTFT, x_2(k-1) - FT, 0), \text{clip}(x_2(k-1) + FT, x_2(k-1) + HFT, 0), x_2^*(k)) \quad (4b)$$

$$x_1(k) := x_1(k-1) + Tx_2(k) \quad (4c)$$

$$\text{RETURN } x_1(k) \text{ and } x_2(k), \quad (4d)$$

where  $T$  is the sampling period, and  $\Phi()$  and  $\text{clip}()$  are functions given as follows:

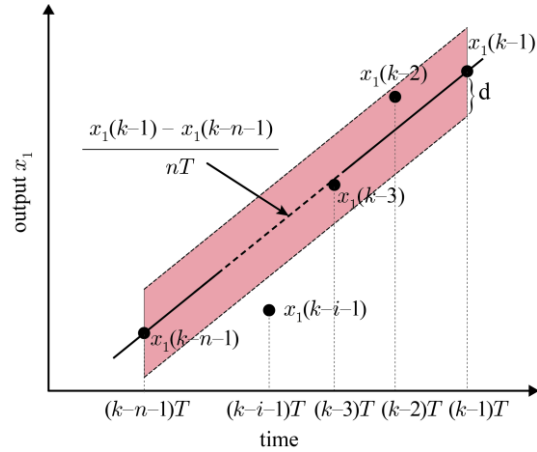


Figure 2. Windowing in AW-PSMF.

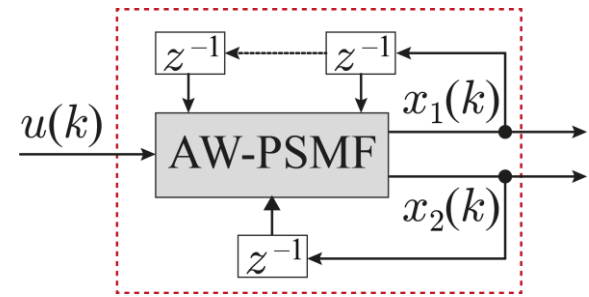


Figure 3. Block diagram of AW-PSMF.

$$\Phi(z) \triangleq \text{sgn}(z)(\sqrt{1+2|z|} - 1) \quad (5)$$

$$\text{clip}(a, b, z) \triangleq \begin{cases} b & \text{if } z > 0 \\ z & \text{if } z \in [a, b] \\ a & \text{if } z < 0. \end{cases} \quad (6)$$

Here,  $a < b$ , and  $x_2^*$  is an intermediate variable, which is followed by  $x_2$  under constraint of  $|(x_2(k) - x_2(k-1))| / T$ .

After the proposal of PSMF, in [10] Jin *et al.* presented an extension version of PSMF by introducing an adaptive window, of which window size is adaptively changed for realizing the largest window size that optimizes the trade-off between the filtering smoothness and the delay suppression. Specifically, the complete algorithm of the modified version of PSMF, which is named as AW-PSMF, is given as follows:

### Algorithm AW - PSMF

$$\text{FOR } n \in \{1, \dots, \min(k+1, N_{\max})\} \quad (7a)$$

$$a := (x_1(k-1) - x_1(k-n-1)) / (nT) \quad (7b)$$

$$\text{FOR } i \in \{1, \dots, n\} \quad (7c)$$

$$e := x_1(k-i-1) - x_1(k-1) + iTa \quad (7d)$$

$$\text{IF } |e| > C; \text{ EXIT LOOP} \quad (7e)$$

$$\text{END FOR} \quad (7f)$$

**IF**  $i < n$ ; **EXIT LOOP** (7g)

**END FOR** (7h)

$$x_2^*(k) := nFT\Phi\left(\frac{u(k) - x_1(k-n)}{n^2 FT^2}\right) \quad (7i)$$

$$x_2(k) := \text{clip}(\text{clip}(x_2(k-1) - HTFT, x_2(k-1) - FT, 0), \text{clip}(x_2(k-1) + FT, x_2(k-1) + HFT, 0), x_2^*(k)) \quad (7j)$$

$$x_1(k) := x_1(k-1) + Tx_2(k) \quad (7k)$$

**RETURN**  $x_1(k)$  and  $x_2(k)$ , (7l)

where  $N_{\max}$  and  $d$  are parameters that should be chosen appropriately.

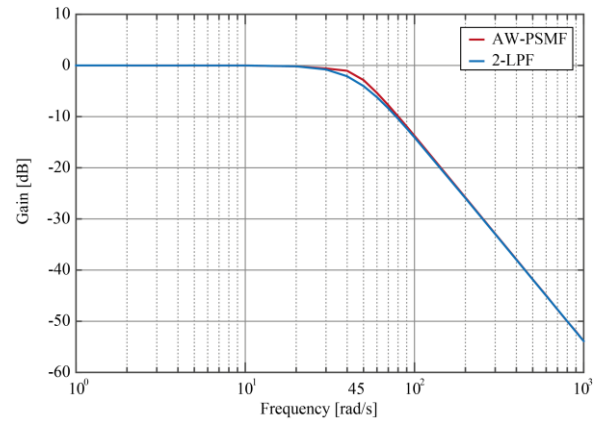
Figure 2. shows block diagram of AW-PSMF. In AW-PSMF, the previous outputs are used for windowing, as shown in Figure 3.. Specifically, AW-PSMF checks whether all previous outputs in the window are inside the area determined by the two end-outputs  $x_1(k)$  and  $x_1(k-n-1)$  and the constant  $d$ . If it is the case, the window size  $n$  is further increased for obtaining smoother output. The increase of  $n$  is continued until at least one previous output in the window lies outside the area or  $n$  reaches its maximum value  $N_{\max}$ . After that, the last  $n$  value is applied for determining  $x_2^*(k)$ , which is an intermediate variable, and then  $x_2(k)$  is determined to follow  $x_2^*(k)$  under constraint of  $|(x_2(k) - x_2(k-1))|/T$ .

### 3 Frequency domain analysis of AW-PSMF

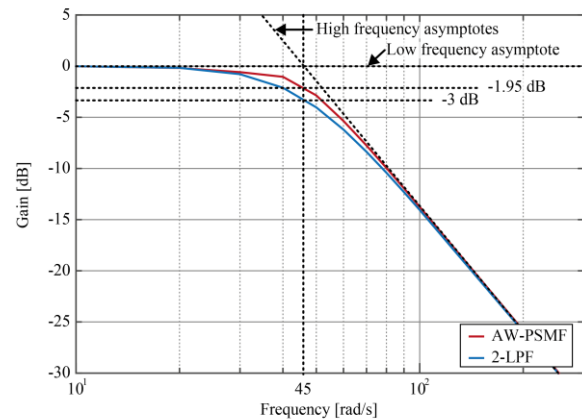
This section analysis the frequency domain behaviour of AW-PSMF by using the Bode plot. It should be mentioned that, due to the nonlinearity of AW-PSMF, the transfer function method cannot be applied here for obtaining Bode plot of AW-PSMF. Thus, as an alternative way, the section applies the Describing Function method [11], which takes into account the fundamental harmonic component of a nonlinear system's response. In this section, sampling period  $T = 0.001$  s is used.

Figure 4. shows Bode plot of AW-PSMF with parameters  $F = 1000$ ,  $H = 5$ ,  $N_{\max} = 10$  and  $d = 0.0001$  for the input signal  $u = \sin(\omega t)$ , where the frequency  $\omega$  changes from 1 rad/s to 1000 rad/s. For comparison, the Bode plot of 2-LPF with cutoff frequency  $\omega_c = 45$  rad/s is also shown in Figure 4. Here, the term 'cutoff frequency' refers to the intersect point of low and high frequency asymptotes, and the cutoff frequency  $\omega_c$  of 2-LPF is chosen so that the gain plot of 2-LPF is as close as possible to that of AW-PSMF.

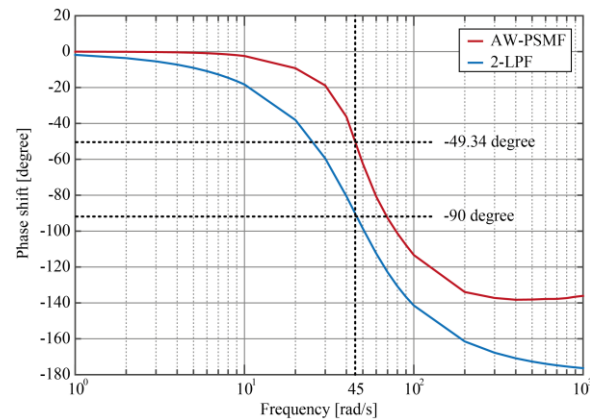
The gain plot shows that the high frequency asymptote of AW-PSMF is approximately -40 dB/decade, which is the same as that of 2-LPF. However, at cutoff frequency, the gain of AW-PSMF is -1.95 dB, whereas that of 2-LPF is -3 dB. It is known that the gain



(a) Gain plot



(b) Enlarged view of (a)



(c) Phase plot

**Figure 4.** Bode plots of AW-PSMF with  $F = 1000$ ,  $H = 5$ ,  $N_{\max} = 10$  and  $d = 0.0001$  and 2-LPF with

plots of Butterworth low-pass filters are the flattest at cutoff frequencies among all linear filters. Thus, it can be concluded that the gain characteristics of AW-PSMF is better than those of all linear filters.

The phase plot shows that the phase shift of AW-PSMF at cutoff frequency is -49.34 degree, whereas that of 2-LPF is -90 degree. In addition, one can observe that the maximum phase shifts of around -140 degree. This is smaller than that of 2-LPF, of which value is -180 degree. Thus, it can be said that the phase characteristics of AW-PSMF is advantageous over that of 2-LPF.

Figure 5. illustrates the comparison between AW-PSMF and 2-LPF in the case where the frequency  $\omega$  of

input  $u = \sin(\omega t)$  changes from 10 rad/s to 20 rad/s at 1.5 s, and then changes again to 30 rad/s at 2.8 s. It is shown that AW-PSMF produced larger gain but smaller phase shift than 2-LPF does for all three input frequencies.

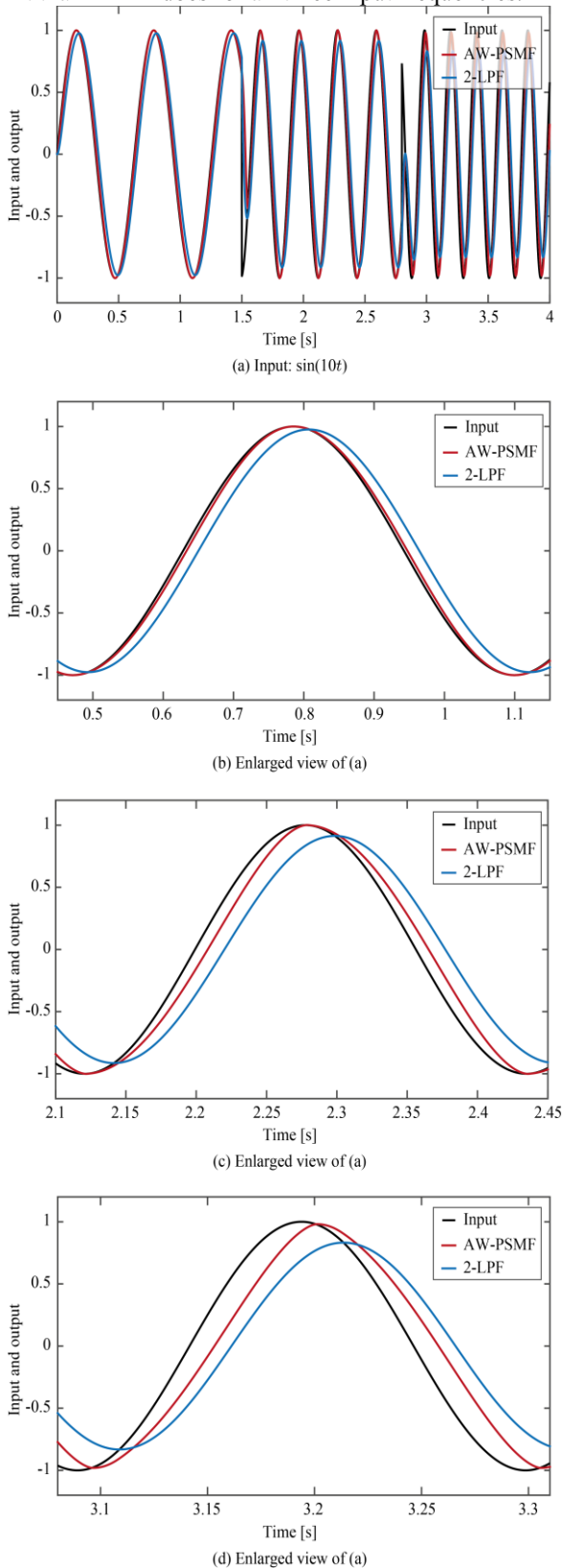


**Figure 5.** Input  $u = \sin(\omega t)$  and outputs of AW-PSMF with  $F = 1000$ ,  $H = 5$ ,  $N_{\max} = 10$  and  $d = 0.0001$  and 2-LPF with  $\omega_{cf} = 45$  rad/s. Here, the frequency of input changes from 10

rad/s to 20 rad/s at 1.5 s, and then changes again to 30 rad/s at 2.8 s rad/s.

## 4 Conclusions

This paper has analysed a frequency domain performance of AW-PSMF by using the Describing Function method. The analysis results show that AW-PSMF has similar gain characteristics to that of 2-LPF, AW-PSMF produces flatter gain behaviour than 2-LPF does at cutoff frequency.

In addition, AW-PSMF produces smaller phase lag (-49.34 degree at cutoff frequency, maximum -140 degree) than 2-LPF (-90~degree at cutoff frequency, maximum -180 degree) does. Thus, it can be concluded that AW-PSMF has better gain and phase characteristics than 2-LPF.

## References

1. Gallagher NJ, Gary LW. A theoretical analysis of the properties of median filters. *IEEE Trans Acoustics, Speech and Signal Processing*. 1981; 29(6):1136-1141.
2. Moshnyaga VG, Hashimoto K. An efficient implementation of 1-D median filter. In: *Proc. 52nd IEEE Int. Midwest Symp. Circuits and Systems*. 2009. p. 451--454.
3. Welch G, Bishop G. An introduction to the Kalman filter. Department of Computer Science, University of North Carolina. 1995. Tech Rep TR95-041.
4. Lightcap CA, Banks SA. An extended Kalman filter for real-time estimation and control of a rigid-link flexible-joint manipulator. *IEEE Trans Control Systems Technology*. 2010; 18(1):91-103.
5. Levant A. Robust exact differentiation via sliding mode technique. *Automatica*. 1998; 34(3):379-384.
6. Moreno JA, Osorio M. A Lyapunov approach to second-order sliding mode controllers and observers. In: *Proc. 47th IEEE Conf. Decision and Control*. 2006. p. 2856-2861.
7. Han JQ, Wang W. Nonlinear tracking-differentiator. *J. System Science and Mathematical Science*. 1994; 14(2):177-183. (in Chinese).
8. Emaru T, Tsuchiya T. Research on estimating smoothed value and differential value by using sliding mode system. *IEEE Trans Robotics and Automation*. 2003; 19(3):391-402.
9. Jin S, Kikuuwe R, Yamamoto M. A Realtime quadratic sliding mode filter for removing noise. In: *Proc. 2011 Robotics and Mechatronics Conf. of The Japan Society of Mechanical Engineers*. 2011. p. 1P1-F03.
10. Jin S, Kikuuwe R, Yamamoto M. Discrete-time velocity estimator basedon sliding mode and adaptive windowing. In: *Proc. 2012 IEEE/SICE Int. Symposium on System Integration*. 2012. p.835-841.
11. Khalil HK. *Nonlinear Systems*, 3rd edition. 2002.